Inorg. Chem. **2000,** *39,* 967−974

Structural Studies of the [Tris(imidazolyl)phosphine]metal Nitrate Complexes $\{[\mathrm{Pim}^{\mathrm{Pr^i,Bu^t}}]\mathrm{M(NO_3)}\}^+$ (M = Co, Cu, Zn, Cd, Hg): Comparison of Nitrate-Binding Modes in Synthetic Analogues of Carbonic Anhydrase

Clare Kimblin, Vincent J. Murphy, Tony Hascall, Brian M. Bridgewater, Jeffrey B. Bonanno, and Gerard Parkin*

Department of Chemistry, Columbia University, New York, New York 10027

Received June 15, 1999

X-ray diffraction studies on a series of cationic divalent metal nitrate complexes supported by the tris(1-isopropyl-4-*tert*-butylimidazolyl)phosphine ligand, $\{[\mathrm{Pim}^{\mathrm{Pr^i,Bu^t}}]\mathrm{M(NO_3)}\}^+$ (M = Co, Cu, Zn, Cd, Hg), demonstrate that the nitrate ligand coordination mode is strongly dependent upon the metal. With the exception of that for the $\mathrm{Hg^{II}}$ derivative, the nitrate ligand coordination modes correlate with the activities of metal-substituted carbonic anhydrases, such that the only $\mathrm{M^{II}}$-carbonic anhydrases which exhibit significant activity, i.e., the Zn and Co species, are those for which the $\{[\mathrm{Pim}^{\mathrm{Pr^i,Bu^t}}]\mathrm{M(NO_3)}\}^+$ complexes possess strongly asymmetric nitrate ligands. This trend supports the notion that access to a unidentate, rather than a bidentate, bicarbonate intermediate may be a critical requirement for significant carbonic anhydrase activity. Interestingly, the nitrate coordination modes in the series of group 12 complexes, $\{[\mathrm{Pim}^{\mathrm{Pr^i,Bu^t}}]\mathrm{M(NO_3)}\}^+$ (M = Zn, Cd, Hg), do not exhibit a monotonic periodic trend: the bidenticity is greater for the cadmium complex than for either the zinc or mercury complexes. Since $\mathrm{Hg^{II}}$-carbonic anhydrase is inactive, the correlation between nitrate coordination mode and enzyme activity is anomalous for the mercury complex. Therefore, it is suggested that the inactivity of $\mathrm{Hg^{II}}$-carbonic anhydrase may be a consequence of the reduced tendency of the mercury center in $\mathrm{Hg^{II}}$-carbonic anhydrase to bind water.

Introduction

Carbonic anhydrase is the zinc enzyme that catalyzes the hydration of carbon dioxide in both plants and animals (eq 1).[1]

$$\mathrm{CO_2 + H_2O \rightleftarrows HCO_3^- + H^+} \qquad (1)$$

X-ray diffraction studies have demonstrated that the active site of the enzyme is comprised of a distorted tetrahedral zinc center which is bound to the protein by the imidazole groups of three histidine residues; the fourth coordination site on zinc is occupied by either a water molecule or a hydroxide ligand, depending upon pH.[2,3] The essential features of the catalytic cycle involve sequentially (i) deprotonation of zinc-bound water to give the active hydroxide $[\mathrm{(His)_3Zn{-}OH}]^+$, (ii) nucleophilic attack of the hydroxide ligand on $\mathrm{CO_2}$, giving the zinc bicarbonate derivative $[\mathrm{(His)_3Zn{-}OCO_2H}]^+$, and (iii) displacement of the bicarbonate ligand by water (Scheme 1).[1,2]

Scheme 1

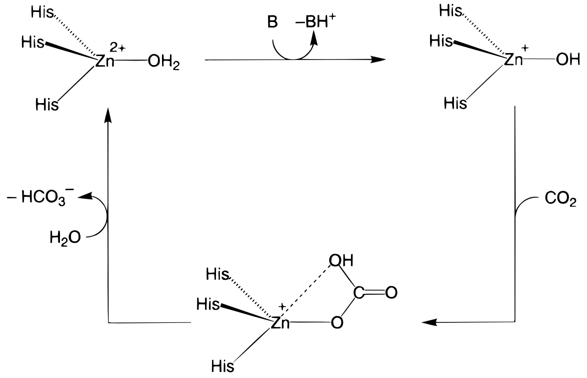

In addition to studies performed on the native enzyme itself, insight into the nature of the active site and the mechanism of action of carbonic anhydrase has been obtained by an investigation of the properties of various metal-substituted enzymes.[4,5] The importance of such studies on metal-substituted carbonic anhydrase is two-fold. Firstly, the poor spectroscopic properties of $\mathrm{Zn^{II}}$ mean that it is difficult to obtain information concerning the structure of the active site and the nature of intermediates.[6] Substitution by divalent metal ions which have useful spectro-

---

(1) (a) Bertini, I.; Luchinat, C. In *Bioinorganic Chemistry*; Bertini, I., Gray, H. B., Lippard, S. J., Valentine, J., Eds.; University Science Books, Mill Valley, CA, 1994. (b) Botre, F., Gros, G., Storey, B. T., Eds. *Carbonic Anhydrase*; VCH: New York, 1991. (c) Christianson, D. W. *Adv. Protein Chem.* **1991**, *42*, 281−355. (d) Silverman, D. N.; Lindskog, S. *Acc. Chem. Res.* **1988**, *21*, 30−36. (e) Dodgson, S. J., Tashian, R. E., Gros, G., Carter, N. D., Eds.; *The Carbonic Anhydrases*; Plenum Publishing Corporation, 1991. (f) Lindskog, S. *Pharmacol. Ther.* **1997**, *74*, 1−20.

(2) (a) Håkansson, K.; Carlsson, M.; Svensson, L. A.; Liljas, A. *J. Mol. Biol.* **1992**, *227*, 1192−1204. (b) Eriksson, A. E.; Jones, A. T.; Liljas, A. *Proteins* **1988**, *4*, 274−282. (c) Nair, S. K.; Christianson, D. W. *J. Am. Chem. Soc.* **1991**, *113*, 9455−9458. (d) Hartmann, M.; Merz, K. M.; van Eldik, R.; Clark, T. *J. Mol. Modeling* **1998**, *4*, 355−365.

(3) For a review of zinc-binding sites in enzymes, see: Alberts, I. L.; Nadassy, K.; Wodak, S. J. *Protein Sci.* **1998**, *7*, 1700−1716.

(4) (a) Williams, R. J. P. *J. Mol. Catal.* **1985**, *30*, 1−26. (b) Bertini, I.; Luchinat, C.; Viezzoli, M. S. In *Zinc Enzymes*; Bertini, I., Luchinat, C., Maret, W., Zeppezauer, M., Eds.; *Progress in Inorganic Biochemistry and Biophysics*, Vol. 1; Birkhäuser: Boston, MA, 1986; Chapter 3. (c) Lindskog, S.; Nyman, P. O.; *Biochim Biophys. Acta* **1964**, *85*, 462−474.

(5) (a) Håkansson, K.; Wehnert, A.; Liljas, A. *Acta Crystallogr.* **1994**, *D50*, 93−100. (b) Håkansson, K.; Wehnert, A. *J. Mol. Biol.* **1992**, *228*, 1212−1218. (c) Liljas, A.; Carlsson, M.; Håkansson, K.; Lindahl, M.; Svensson, L. A.; Wehnert, A. *Philos. Trans. R. Soc. London, Ser. A* **1992**, *340*, 301−309.

(6) Sigel, H.; Martin, R. B. *Chem. Soc. Rev.* **1994**, *23*, 83−91.

10.1021/ic990682v CCC: $19.00

scopic probes, e.g. Co^{II} (UV−vis) and Cd^{II} (NMR), therefore allows structural information on the metal-substituted carbonic anhydrase active site to be obtained. Secondly, the difference in activity of the various metal-substituted enzymes should afford insight into the mechanism of action of the enzyme, as illustrated by some recent theoretical calculations.[7] However, the use of metal ion substitution to provide insight of the type indicated above depends critically on our understanding of the chemistry of various metal ions in coordination environments that are closely related to the enzyme active site. For this reason, it is important to discern the chemistry of metals in such coordination environments. Therefore, in this paper we describe the structural changes in the coordination mode of a nitrate ligand that occur as a function of the metal in a series of complexes incorporating a tris(imidazolyl)phosphine ligand which mimics the three imidazole residues at the active site of carbonic anhydrase. Some of these results have been previously communicated.[8,9]

Results and Discussion

We recently described the application of the sterically demanding tris(1-isopropyl-4-*tert*-butylimidazolyl)]phosphine ligand $[\mathrm{Pim}^{\mathrm{Pr^i,Bu^t}}]$[10,11] in the preparation of a synthetic analogue for carbonic anhydrase. Specifically, $\{[\mathrm{Pim}^{\mathrm{Pr^i,Bu^t}}]\mathrm{ZnOH}\}(\mathrm{ClO_4})$, the first structurally characterized monomeric zinc hydroxide complex supported by imidazole functionalities, was synthesized by reaction of $[\mathrm{Pim}^{\mathrm{Pr^i,Bu^t}}]$ with $\mathrm{Zn(ClO_4)_2{\cdot}6H_2O}$.[8] A critical step in the mechanism of action of carbonic anhydrase involves the formation of a bicarbonate intermediate,[1] and we have previously suggested that the nature of the interaction between the metal center and the bicarbonate ligand is likely to play an important role in determining the efficiency of the catalytic cycle.[12,13] Specifically, a metal center that increases the tendency to form a bidentate bicarbonate intermediate is expected to inhibit the mechanism of action of carbonic anhydrase by virtue of the notion that displacement of a bidentate ligand by water would be less favored than that for the corresponding unidentate ligand.[14,15] A critical requirement for carbonic anhydrase activity may therefore be the accessibility of a unidentate, rather than a bidentate, bicarbonate intermediate.[16]

Metal bicarbonate complexes, however, are rare, and it is presently not possible to study the variation of bicarbonate coordination mode as a function of metal in environments which mimic the active sites of zinc enzymes.[17,18] For example, zinc bicarbonate complexes are generally unstable with respect to loss of $\mathrm{CO_2}$, as exemplified by the rapid conversion of the tris(3-*tert*-butyl-5-methylpyrazolyl)hydroborato complex $[\mathrm{Tp}^{\mathrm{Bu^t,Me}}]\mathrm{Zn(OCO_2H)}$ to $[\mathrm{Tp}^{\mathrm{Bu^t,Me}}]\mathrm{ZnOH}$; furthermore an attempt to isolate $[\mathrm{Tp}^{\mathrm{Bu^t,Me}}]\mathrm{Zn(OCO_2H)}$ in the solid state by crystallization under a $\mathrm{CO_2}$ atmosphere yielded only a dinuclear bridging carbonate complex, $\{[\mathrm{Tp}^{\mathrm{Bu^t,Me}}]\mathrm{Zn}\}_2(\mu\text{-}\eta^1,\eta^1\text{-}\mathrm{CO_3})$.[12,19,20] In view of this paucity of metal bicarbonate complexes, we have proposed that the nitrate ligand may be employed as a probe to provide an indication of the structural variations that would be expected for a series of bicarbonate complexes.[12,13] Thus, since bicarbonate and nitrate ligands are isoelectronic and sterically similar, and both ligands can bind metals by either one or two oxygen atoms, the *variation* in nitrate coordination mode for a series of analogous metal complexes is anticipated to correlate with the *trend* observed for analogous bicarbonate complexes.[21]

While the tris(pyrazolyl)hydroborato ligand system $[\mathrm{Tp}^{\mathrm{R,R'}}]$ has been of use in advancing our understanding of the activity of metal-substituted carbonic anhydrases,[13] the $[\mathrm{Tp}^{\mathrm{R,R'}}]$ ligand suffers from the disadvantage that the nitrogen donors are pyrazolyl-based rather than imidazolyl-based. Furthermore, the analogy between the $\{[\mathrm{Tp}^{\mathrm{Bu^t}}]\mathrm{M}^{\mathrm{II}}\}^+$ moieties in the aforementioned model complexes and those in the enzymes, $\{[\mathrm{His}]_3\mathrm{M}^{\mathrm{II}}\}^{2+}$, is limited as a result of the difference in formal charge. Consequently, it is of interest to determine the extent to which nitrate (bicarbonate) coordination is influenced by a

---

(7) (a) Garmer, D. R.; Krauss, M. *J. Am. Chem. Soc.* **1992**, *114*, 6487−6493. (b) Garmer, D. R.; Krauss, M. *Int. J. Quantum Chem.* **1992**, *42*, 1469−1477. (c) Garmer, D. R.; Krauss, M. *J. Am. Chem. Soc.* **1993**, *115*, 10247−10257. (d) Vedani, A.; Huhta, D. W. *J. Am. Chem. Soc.* **1990**, *112*, 4759−4767.

(8) Kimblin, C.; Allen, W. E.; Parkin, G. *J. Chem. Soc., Chem. Commun.* **1995**, 1813−1815.

(9) Kimblin, C.; Murphy, V. J.; Parkin, G. *J. Chem. Soc., Chem. Commun.* **1996**, 235−236.

(10) Sorrell, T. N.; Allen, W. E.; White, P. S. *Inorg. Chem.* **1995**, *34*, 952−960.

(11) Abbreviations: tris(2-imidazolyl)phosphines are represented by the abbreviation $[\mathrm{Pim}^{\mathrm{R,R'}}]$, with the 1- and 4-alkyl substituents listed respectively as superscripts; tris(1-pyrazolyl)hydroborato ligands are represented by the abbreviation $[\mathrm{Tp}^{\mathrm{R,R'}}]$, with the 3- and 5-alkyl substituents listed respectively as superscripts.

(12) Looney, A.; Han, R.; McNeill, K.; Parkin, G. *J. Am. Chem. Soc.* **1993**, *115*, 4690−4697.

(13) (a) Han, R.; Parkin, G. *J. Am. Chem. Soc.* **1991**, *113*, 9707−9708. (b) Han, R.; Looney, A.; McNeill, K.; Parkin, G.; Rheingold, A. L.; Haggerty, B. S. *J. Inorg. Biochem.* **1993**, *49*, 105−121. (c) Looney, A.; Saleh, A.; Zhang, Y. H.; Parkin, G. *Inorg. Chem.* **1994**, *33*, 1158−1164.

(14) Other researchers have also endorsed this opinion: (a) Kitajima, N.; Hikichi, S.; Tanaka, M.; Moro-oka, Y. *J. Am. Chem. Soc.*, **1993**, *115*, 5496−5508. (b) Zhang, X.; van Eldik, R. *Inorg. Chem.* **1995**, *34*, 5606−5614.

(15) Theoretical calculations also consider that displacement of bicarbonate by water occurs via a unidentate bicarbonate intermediate. See, for example: Jacob, O.; Cardenas, R.; Tapia, O. *J. Am. Chem. Soc.* **1990**, *112*, 8692−8705.

(16) This suggestion is not intended to imply that the nature of the bicarbonate intermediate is the most important factor in influencing the activity of metal-substituted carbonic anhydrases. Obviously factors such as the pK_a of the coordinated water are critical to the enzyme activity. See, for example, ref 7.

(17) Although rare, structurally characterized mononuclear bicarbonate complexes are known for metals such as Co,[17a,b] Cu,[17c] Cd,[17d] W,[17e] Ru,[17f] Rh,[17g,h] Pd[17i,j] and Pt.[17k] However, no such complexes are known for zinc. Mixed bicarbonate-carbonate species, $\mathrm{NaA_2\{Zn_2[H(CO_3)_2](CO_3)_2(H_2O)_2\}}$ (A = K, Rb), are nevertheless known in the solid state.[17l] (a) Döring, M.; Meinert, M.; Uhlig, E.; Dahlenburg, L.; Fawzi, R. *Z. Anorg. Allg. Chem.* **1991**, *598/599*, 71−82. (b) Baxter, K. E.; Hanton, L. R.; Simpson, J.; Vincent, B. R.; Blackman, A. G. *Inorg. Chem.* **1995**, *34*, 2795−2796. (c) Latos-Grazynski, L.; Lisowski, J.; Olmstead, M. M.; Balch, A. L. *J. Am. Chem. Soc.* **1987**, *109*, 4428−4429. (d) Ito, H.; Ito, T. *Acta Crystallogr.* **1985**, *C41*, 1598−1602. (e) Darensbourg, D. J.; Jones, M. L. M.; Reibenspies, J. H. *Inorg. Chem.* **1996**, *35*, 4406−4413. (f) Romero, A.; Santos, A.; Vegas, A. *Organometallics* **1988**, *7*, 1988−1983. (g) Hossain, S. F.; Nicholas, K. M.; Teas, C. L.; Davis, R. E. *J. Chem. Soc., Chem. Commun.* **1981**, 268−269. (h) Yoshida, T.; Thorn, D. L.; Okano, T.; Ibers, J. A.; Otsuka, S. *J. Am. Chem. Soc.* **1979**, *101*, 4212−4221. (i) Crutchley, R. J.; Powell, J.; Faggiani, R.; Lock, C. J. L. *Inorg. Chim. Acta* **1977**, *24*, L15−L16. (j) Ganguly, S.; Mague, J. T.; Roundhill, D. M. *Inorg. Chem.* **1992**, *31*, 3831−3835. (k) Ito, M.; Ebihara, M.; Kawamura, T. *Inorg. Chim. Acta* **1994**, *218*, 199−202. (l) Zheng, Y. Q.; Adam, A. *Z. Naturforsch.* **1995**, *50b*, 1185−1194.

(18) Furthermore, alkyl carbonate complexes are also rare. For examples of zinc and cadmium derivatives, see: (a) Kato, M.; Ito, T. *Inorg. Chem.* **1985**, *24*, 509−514. (b) Alsfasser, R.; Ruf, M.; Trofimenko, S.; Vahrenkamp, H. *Chem. Ber.* **1993**, *126*, 703−710. (c) Ruf, M.; Vahrenkamp, H. *Inorg. Chem.* **1996**, *35*, 6571−6578. (d) Kato, M.; Ito, T. *Bull. Chem. Soc. Jpn.* **1986**, *59*, 285−294. (e) Reference 17d.

(19) For a related complex with an asymmetrically bridged carbonate ligand, $\{[\mathrm{Tp}^{\mathrm{Pr^i}_2}]\mathrm{Zn}\}_2(\mu\text{-}\eta^1,\eta^2\text{-}\mathrm{CO_3})$, see refs 12 and 14a.

(20) For examples in zinc chemistry where bicarbonate species have been proposed as reactive intermediates, see: (a) Reference 14b. (b) Zhang, X.; van Eldik, R.; Koike, T.; Kimura, E. *Inorg. Chem.* **1993**, *32*, 5749−5755.

(21) We emphasize that this statement does not imply that a nitrate ligand coordination mode will be identical to that in a corresponding bicarbonate complex. Rather, it is suggested that, for a group of closely related nitrate and bicarbonate complexes, the variations in denticity will be similar for the two series.

Scheme 2

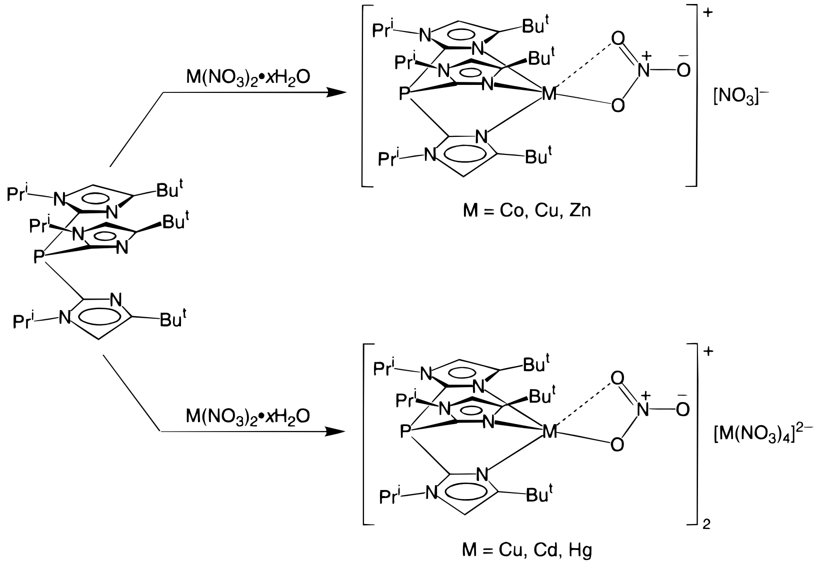

metal for the more relevant tris(imidazolyl)phosphine system. For this reason, we have synthesized and structurally characterized by X-ray diffraction a series of [tris(1-isopropyl-4-*tert*-butylimidazolyl)phosphine]metal nitrate complexes, $\{[\mathrm{Pim}^{\mathrm{Pr^i,Bu^t}}]\mathrm{M(NO_3)}\}^+$.

Syntheses of $\{[\mathrm{Pim}^{\mathrm{Pr^i,Bu^t}}]\mathrm{M(NO_3)}\}^+$ (M = Co, Cu, Zn, Cd, Hg). The nitrate complexes $\{[\mathrm{Pim}^{\mathrm{Pr^i,Bu^t}}]\mathrm{M(NO_3)}\}^+$ (M = Co, Cu, Zn, Cd, Hg) are readily obtained by direct addition of $[\mathrm{Pim}^{\mathrm{Pr^i,Bu^t}}]$ to the appropriate metal nitrate, as illustrated in Scheme 2. Depending upon the metal, the complexes $\{[\mathrm{Pim}^{\mathrm{Pr^i,Bu^t}}]\mathrm{M(NO_3)}\}^+$ are isolated either with $(\mathrm{NO_3})^-$ as the counteranion (M = Co, Cu, Zn) or with $[\mathrm{M(NO_3)_4}]^{2-}$ as the counterion (M = Cu, Cd, Hg).[22]

Structures of $\{[\mathrm{Pim}^{\mathrm{Pr^i,Bu^t}}]\mathrm{M(NO_3)}\}^+$ (M = Co, Cu, Zn, Cd, Hg). The structures of $\{[\mathrm{Pim}^{\mathrm{Pr^i,Bu^t}}]\mathrm{M(NO_3)}\}^+$ (M = Co, Cu, Zn, Cd, Hg) have been determined by X-ray diffraction and are illustrated in Figures 1−6, with selected bond lengths listed in Tables 1−6, from which it is evident that the nitrate ligand binding mode varies considerably among the complexes. According to the asymmetry of the interaction, the coordination mode of a nitrate ligand may be classified as bidentate, anisobidentate, or unidentate;[23,24] the pertinent criteria commonly used for assigning these coordination modes are summarized in Figure 7 and Table 7.[23] The salient data for assigning the coordination modes within $\{[\mathrm{Pim}^{\mathrm{Pr^i,Bu^t}}]\mathrm{M(NO_3)}\}^+$ are summarized in Table 8 and indicate that bidenticity increases in the sequence Zn < Hg < Co < Cu ∼ Cd.

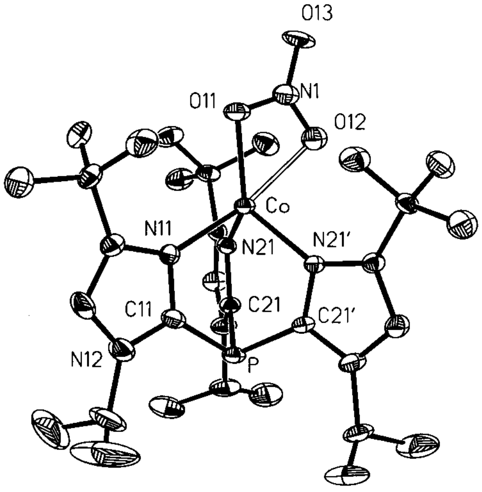

Figure 1. Molecular structure of $\{[\mathrm{Pim}^{\mathrm{Pr^i,Bu^t}}]\mathrm{Co(NO_3)}\}(\mathrm{NO_3})$. (Only the cation is shown for clarity).

The notion that the variation in nitrate coordination mode in these synthetic analogues reflects the trend in bicarbonate coordination mode is provided by X-ray diffraction studies on the enzymes. Specifically, the X-ray structure of human CA I complexed with bicarbonate indicates that the bicarbonate ligand is coordinated to zinc in a unidentate fashion with inequivalent Zn−O bond lengths (1.8 and 3.1 Å),[25−27] whereas the bicarbonate ligand in cobalt carbonic anhydrase II binds more symmetrically (2.39 and 2.44 Å).[28,29]

---

(22) In this regard, it is worth noting that $[\mathrm{Co(NO_3)_4}]^{2-}$ [22a] and $[\mathrm{Zn(NO_3)_4}]^{2-}$ [22b−d] counterions have been structurally characterized previously, although they are not found in the complexes reported upon herein. The structures of $[\mathrm{Cu(NO_3)_4}]^{2-}$ [22e,f] and $[\mathrm{Cd(NO_3)_4}]^{2-}$ [22g] have also been reported. (a) Bergman, J. G., Jr.; Cotton, F. A. *Inorg. Chem.* **1966**, *5*, 1208−1213. (b) Bellitto, C.; Gastaldi, L.; Tomlinson, A. A. G. *J. Chem. Soc., Dalton Trans.* **1976**, 989−992. (c) Turonek, M. L.; Moore, P.; Clase, H. J.; Alcock, N. W. *J. Chem. Soc., Dalton Trans.* **1995**, 3659−3666. (d) Drummond, J.; Wood, J. S. *J. Chem. Soc. A.* **1970**, 226−232. (e) King, T. J.; Morris, A. *Inorg. Nucl. Chem. Lett.* **1974**, *10*, 237−241. (f) Xiao-Yan, L.; Ya-Juan, W. *Acta Chim. Sin. (Engl. Ed.)* **1996**, *54*, 431−439. (g) Alcock, N. W.; Curzon, E. H.; Moore, P.; Pierpoint, C. *J. Chem. Soc., Dalton Trans* **1984**, 605−610.

(23) Kleywegt, G. J.; Wiesmeijer, W. G. R.; Van Driel, G. J.; Driessen, W. L.; Reedijk, J.; Noordik, J. H. *J. Chem. Soc., Dalton Trans.* **1985**, 2177−2184.

(24) Addison, C. C.; Logan, N.; Wallwork, S. C.; Garner, C. D. *Q. Rev. Chem. Soc.* **1971**, 289−322.

(25) Kumar, V.; Kannan, K. K. *J. Mol. Biol.* **1994**, *241*, 226−232.

(26) The structures of carbonic anhydrase mutants in the presence of bicarbonate have also been reported. See: (a) Xue, Y.; Vidgren, J.; Svensson, L. A.; Liljas, A.; Jonsson, B.-H.; Lindskog, S. *Proteins* **1993**, *15*, 80−87. (b) Xue, Y.; Liljas, A.; Jonsson, B.-H.; Lindskog, S. *Proteins* **1993**, *17*, 93−106.

(27) The nitrate ligand is also observed to bind to the zinc center in carbonic anhydrase with a unidentate mode; however, the Zn−O bond is very long (2.8 Å) and does not displace the water. [27a] Likewise, acetate does not fully displace the water in carbonic anhydrase.[27b] (a) Mangani, S.; Håkansson, K. *Eur. J. Biochem.* **1992**, *210*, 867−871. (b) Håkansson, K.; Briand, C.; Zaitsev, V.; Xue, Y.; Liljas, A. *Acta Crystallogr.* **1994**, *D50*, 101−104.

(28) Håkansson, K.; Wehnert, A. *J. Mol. Biol.* **1992**, *228*, 1212−1218.

(29) Furthermore, an EXAFS study on carbonic anhydrase in the presence of bicarbonate has suggested that the zinc center remains four-coordinate, whereas the cobalt derivative is proposed to be five-coordinate. See: Yachandra, V.; Powers, L.; Spiro, T. G. *J. Am. Chem. Soc.* **1983**, *105*, 6596−6604.

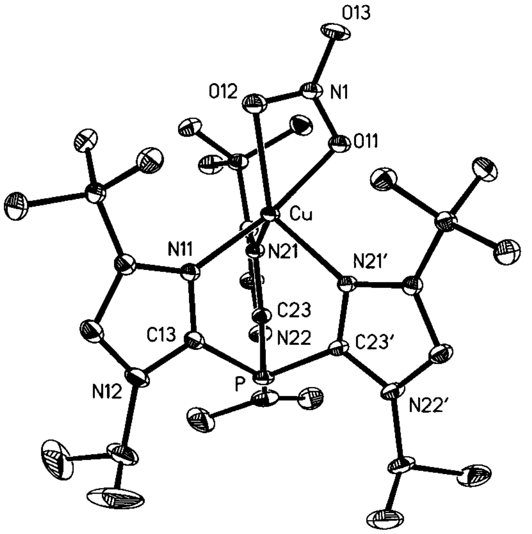

Figure 2. Molecular structure of $\{[\mathrm{Pim}^{\mathrm{Pr^i,Bu^t}}]\mathrm{Cu(NO_3)}\}(\mathrm{NO_3})$. (Only the cation is shown for clarity).

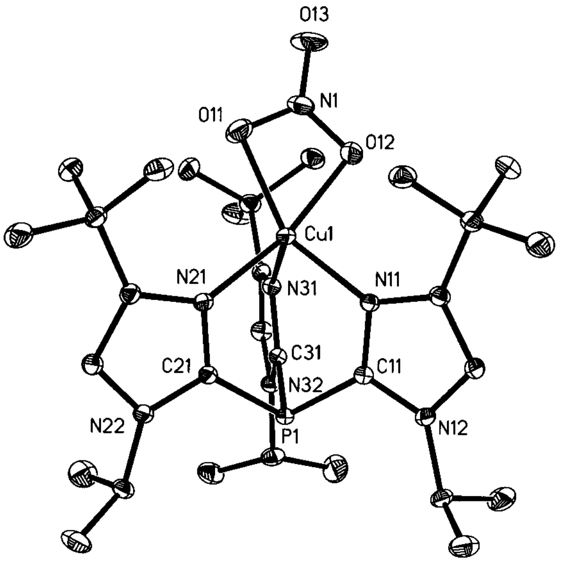

Figure 3. Molecular structure of $\{[\mathrm{Pim}^{\mathrm{Pr^i,Bu^t}}]\mathrm{Cu(NO_3)}\}_2[\mathrm{Cu(NO_3)_4}]$. (Only one of the cations is shown for clarity.)

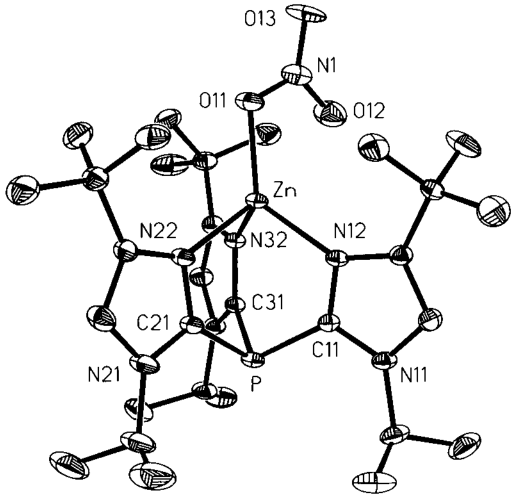

Figure 4. Molecular structure of $\{[\mathrm{Pim}^{\mathrm{Pr^i,Bu^t}}]\mathrm{Zn(NO_3)}\}(\mathrm{NO_3})$. (Only the cation is shown for clarity.)

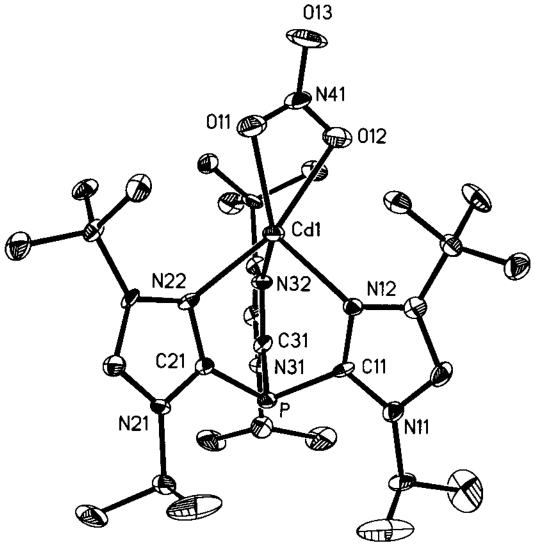

Figure 5. Molecular structure of $\{[\mathrm{Pim}^{\mathrm{Pr^i,Bu^t}}]\mathrm{Cd(NO_3)}\}_2[\mathrm{Cd(NO_3)_4}]$. (Only one of the cations is shown for clarity).

Interestingly, the coordination mode of the nitrate ligand in the zinc, cadmium, and mercury complexes $\{[\mathrm{Pim}^{\mathrm{Pr^i,Bu^t}}]\mathrm{M(NO_3)}\}^+$ (M = Zn, Cd, Hg) does not exhibit a monotonic periodic trend: the bidenticity is greater for cadmium than for either zinc or mercury (Table 8). For example, the asymmetry of the M−O bond lengths alternates as follows: Zn (0.53 Å), Cd (0.13 Å), Hg (0.39 Å). The anomalous behavior of mercury in $\{[\mathrm{Pim}^{\mathrm{Pr^i,Bu^t}}]\mathrm{Hg(NO_3)}\}^+$ with respect to its lighter congener is precedented by comparison of the structures of the silver and gold nitrate complexes $\mathrm{Ag(NO_3)(PPh_3)}$[30] and $\mathrm{Au(NO_3)(PPh_3)}$.[31] In these complexes, Au is two-coordinate and linear, with the nitrate binding in a distinctly unidentate manner [*d*(Au−O) = 2.074(8) and 2.84(1) Å], while Ag is four-coordinate by virtue of both a bidentate interaction [*d*(Ag−O) = 2.438(7) and 2.628(7) Å] and a supplementary interaction [*d*(Ag−O) = 2.363(7) Å] with an adjacent molecule.

Since there are no $[\mathrm{Hg(NO_3)_4}]^{2-}$ derivatives listed in the Cambridge Structural Database,[32] the structural characterization of $\{[\mathrm{Pim}^{\mathrm{Pr^i,Bu^t}}]\mathrm{Hg(NO_3)}\}_2[\mathrm{Hg(NO_3)_4}]$ makes it worthwhile to compare the structures of the entire series of anions $[\mathrm{M(NO_3)_4}]^{2-}$ (M = Zn, Cd, Hg). On the basis of the data presented in Table 9, it is evident that the asymmetry of the interaction (as judged by the M−O bond lengths) is greatest for the zinc derivative, which is in accord with the observations made for the cations $\{[\mathrm{Pim}^{\mathrm{Pr^i,Bu^t}}]\mathrm{M(NO_3)}\}^+$. Interestingly, the nitrate ligands in the cadmium anion $[\mathrm{Cd(NO_3)_4}]^{2-}$ have been observed to adopt several different coordination modes; the tetraazacyclohexadecane complex $[\{\mathrm{MeNC_3H_6}\}_4\mathrm{Cd(NO_3)}]_2[\mathrm{Cd(NO_3)_4}]$ is of particular note because it contains two crystallographically independent $[\mathrm{Cd(NO_3)_4}]^{2-}$ anions which possess different Cd−O bond lengths (Table 9). It is also noteworthy that the bidentate nitrate coordination mode in $[\mathrm{Hg(NO_3)_4}]^{2-}$ contrasts with the unidentate coordination mode in the counterion $\{[\mathrm{Pim}^{\mathrm{Pr^i,Bu^t}}]\mathrm{Hg(NO_3)}\}^+$.

With the exception of that in the mercury complex, the coordination mode of the nitrate ligand in $\{[\mathrm{Pim}^{\mathrm{Pr^i,Bu^t}}]\mathrm{M(NO_3)}\}^+$ correlates reasonably well with the activity of metal-substituted carbonic anhydrases: Zn > Co ≫ Cu ∼ Cd ∼ Hg (Table 10).

---

(30) Stein, R. A.; Knobler, C. *Inorg. Chem.* **1977**, *16*, 242−245.

(31) Wang, J.-C.; Khan, M. N. I.; Fackler, J. P., Jr. *Acta Crytallogr.* **1989**, *C45*, 1008−1010.

(32) Allen, F. H.; Kennard, O. CSD Version 5.17. 3D Search and Research Using the Cambridge Structural Database. *Chem. Des. Autom. News* **1993**, *8* (1), 1, 31−37.

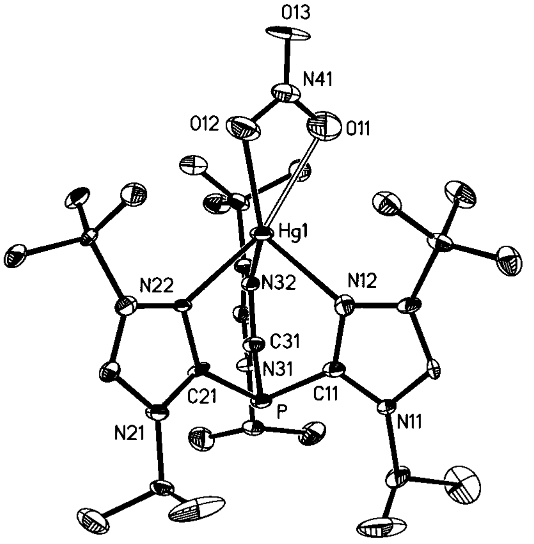

Figure 6. Molecular structure of $\{[Pim^{Pr^i,Bu^t}]Hg(NO_3)\}_2[Hg(NO_3)_4]$. (Only one of the cations is shown for clarity.)

Table 1. Selected Bond Lengths (Å) and Angles (deg) for $\{[Pim^{Pr^i,Bu^t}]Zn(NO_3)\}(NO_3)$

Zn−O(11)	1.986 (4)	Zn−O(12)	2.518 (8)
Zn−N(12)	2.054(4)	Zn−N(22)	2.074(3)
Zn−N(32)	2.048(3)	N(1)−O(11)	1.278(6)
N(1)−O(12)	1.237(8)	N(1)−O(13)	1.217(7)
Zn−O(11)−N(1)	106.8(4)	Zn−O(12)−N(1)	82.4 (8)
O(11)−N(1)−O(12)	115.8(5)	O(11)−Zn−N(12)	121.5(2)
O(11)−Zn−N(22)	111.7(2)	O(11)−Zn−N(32)	124.1(1)
O(11)−N(1)−O(13)	120.3(6)	O(12)−N(1)−O(13)	123.9(5)

Table 2. Selected Bond Lengths (Å) and Angles (deg) for $\{[Pim^{Pr^i,Bu^t}]Co(NO_3)\}(NO_3)$

Co−O(11)	2.019(8)	Co−O(12)	2.289(10)
Co−N(11)	2.074(10)	Co−N(21)	2.084(6)
N(1)−O(11)	1.303(20)	N(1)−O(12)	1.242(16)
N(1)−O(13)	1.210(16)		
Co−O(11)−N(1)	98.8(7)	Co−O(12)−N(1)	88.0(9)
O(11)−N(1)−O(12)	114.2(11)	O(11)−Co−N(11)	110.1(4)
O(11)−Co−N(21)	124.0(2)	O(11)−N(1)−O(13)	120.3(12)
O(12)−N(1)−O(13)	125.5(15)		

Table 3. Selected Bond Lengths (Å) and Angles (deg) for $\{[Pim^{Pr^i,Bu^t}]Cu(NO_3)\}_2[Cu(NO_3)_4]$

Cu(1)−O(11)	2.064(2)	Cu(1)−O(12)	2.0132(19)
Cu(1)−N(11)	1.999(2)	Cu(1)−N(21)	1.984(2)
Cu(1)−N(31)	2.342(2)	N(1)−O(11)	1.261(3)
N(1)−O(12)	1.264(3)	N(1)−O(13)	1.215(3)
Cu(2)−O(21)	1.998(2)	Cu(2)−O(22)	2.148(2)
Cu(2)−N(101)	2.170(2)	Cu(2)−N(111)	1.967(2)
Cu(2)−N(121)	2.055(2)	N(2)−O(21)	1.257(3)
N(2)−O(22)	1.258(3)	N(2)−O(23)	1.211(3)
Cu(1)−O(11)−N(1)	90.99(16)	Cu(1)−O(12)−N(1)	93.24(16)
O(11)−N(1)−O(12)	113.4(2)	O(11)−Cu(1)−N(11)	148.55(10)
O(11)−Cu(1)−N(21)	105.02(9)	O(11)−Cu(1)−N(31)	104.84(10)
O(11)−N(1)−O(13)	123.7(3)	O(12)−N(1)−O(13)	122.9(3)
Cu(2)−O(21)−N(2)	95.85(16)	Cu(2)−O(22)−N(2)	88.81(16)
O(21)−N(2)−O(22)	114.2(2)	O(21)−Cu(2)−N(101)	93.78(9)
O(21)−Cu(2)−N(111)	169.67(9)	O(21)−Cu(2)−N(121)	95.30(8)
O(21)−N(2)−O(23)	122.3(3)	O(22)−N(2)−O(23)	123.5(3)
O(22)−Cu(2)−O(21)	61.11(9)	O(12)−Cu(1)−O(11)	62.36(9)

Table 4. Selected Bond Lengths (Å) and Angles (deg) for $\{[Pim^{Pr^i,Bu^t}]Cu(NO_3)\}(NO_3)$

Cu−O(11)	1.983(4)	Cu−O(12)	2.172(4)
Cu−N(11)	1.983(4)	Cu−N(21)	2.113(3)
N(1)−O(11)	1.267(6)	N(1)−O(12)	1.256(6)
N(1)−O(13)	1.212(6)		
Cu−O(11)−N(1)	96.4(3)	Cu−O(12)−N(1)	87.9(3)
O(11)−N(1)−O(12)	114.5(4)	O(11)−Cu−N(11)	169.84(16)
O(11)−Cu−N(21)	94.35(11)	O(11)−N(1)−O(13)	121.9(5)
O(12)−N(1)−O(13)	123.6(5)		

Table 5. Selected Bond Lengths (Å) and Angles (deg) for $\{[Pim^{Pr^i,Bu^t}]Cd(NO_3)\}_2[Cd(NO_3)_4]$

Cd−O(11)	2.254(9)	Cd−O(12)	2.386(9)
Cd−N(12)	2.265(11)	Cd−N(22)	2.277(9)
Cd−N(32)	2.248(10)	N(41)−O(11)	1.209(13)
N(41)−O(12)	1.242(13)	N(41)−O(13)	1.223(13)
Cd−O(11)−N(41)	97.8(8)	Cd−O(12)−N(41)	90.4(8)
O(11)−N(41)−O(12)	118.0(12)	O(11)−Cd−N(12)	128.8(4)
O(11)−Cd−N(22)	107.7(4)	O(11)−Cd−N(32)	132.3(4)
O(11)−N(41)−O(13)	122.0(13)	O(12)−N(41)−O(13)	119.9(14)

Table 6. Selected Bond Lengths (Å) and Angles (deg) for $\{[Pim^{Pr^i,Bu^t}]Hg(NO_3)\}_2[Hg(NO_3)_4]$

Hg−O(11)	2.61(2)	Hg−O(12)	2.224(14)
Hg−N(12)	2.304(12)	Hg−N(22)	2.262(10)
Hg−N(32)	2.271(11)	N(41)−O(11)	1.25(2)
N(41)−O(12)	1.25(2)	N(41)−O(13)	1.19(2)
Hg−O(11)−N(41)	88.6(12)	Hg−O(12)−N(41)	107.9(12)
O(11)−N(41)−O(12)	113.0(2)	O(11)−Hg−N(12)	104.7(5)
O(11)−Hg−N(22)	161.8(5)	O(11)−Hg−N(32)	104.6(5)
O(11)−N(41)−O(13)	121.2(2)	O(12)−N(41)−O(13)	126(2)

Table 7. Criteria for Assigning Nitrate Coordination Modes[a]

	unidentate	anisobidentate	bidentate
$d_2 - d_1$ Å	>0.6	0.3−0.6	<0.3
$\theta_1 - \theta_2$ deg	>28	14−28	<14

[a] Kleywegt, G. J.; Wiesmeijer, W. G. R.; Van Driel, G. J.; Driessen, W. L.; Reedijk, J.; Noordik, J. H. *J. Chem. Soc., Dalton Trans.* **1985**, 2177−2184.

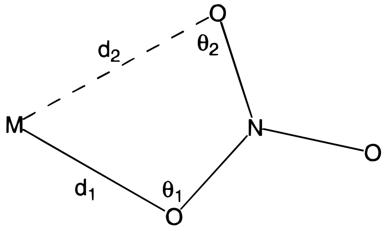

Figure 7. Parameters used for assigning nitrate coordination modes.

Specifically, those metals with almost symmetric bidentate coordination are inactive, whereas those with a significant asymmetry (Zn and Co) are active. This supports the notion that due consideration should be given to the nature of the bicarbonate intermediate of the catalytic cycle.[33] The mercury complex, however, presents a clear anomaly in this correlation: specifically, the nitrate ligand in $\{[Pim^{Pr^i,Bu^t}]Hg(NO_3)\}^+$ is distinctly asymmetric, but yet Hg^{II}-carbonic anhydrase is completely inactive. A possible reason for the inactivity of Hg^{II}-carbonic anhydrase may be that the Hg^{II} center does not bind water efficiently. Support for this suggestion is provided by the fact that an X-ray diffraction study on closely related Hg^{II}-carboxypeptidase A indicates that water does not coordinate to the Hg^{II} center; in preference, tris(hydroxymethyl)aminomethane buffer is proposed to bind.[34] In this regard, the chemistry of

---

(33) A reviewer has suggested that different metals may also influence the nature of a bicarbonate intermediate by modifying the extent to which a bidentate bicarbonate ligand binds via either two oxygen atoms or an oxygen atom and a hydroxyl group, i.e. $M[\eta^2\text{-}O_2COH]$ versus $M[\eta^2\text{-}O(OH)CO]$, and that this in turn may be a reason for the different activities of metal-substituted carbonic anhydrases.

Table 8. Classification of Nitrate Coordination Mode for $\{[\mathrm{Pim}^{\mathrm{Pr^i,Bu^t}}]\mathrm{M(NO_3)}\}^+$

	d_1/Å	d_2/Å	θ_1/deg	θ_2/deg	Δd/Å	$\Delta\theta$/deg	classification
Co	2.019(8)	2.289(10)	98.8(7)	88.0(9)	0.27	10.8	bidentate
Cu[a]	2.013(2)	2.064(2)	93.24(16)	90.99(16)	0.05	2.3	bidentate
	1.998(2)	2.148(2)	95.85(16)	88.81(16)	0.15	7.0	bidentate
Cu[b]	1.983(4)	2.172(4)	96.4(3)	87.9(3)	0.19	8.5	bidentate
Zn	1.986(4)	2.518(8)	106.8(4)	82.4(8)	0.53	24.4	anisobidentate
Cd	2.254(9)	2.386(9)	97.8(8)	90.4(8)	0.13	7.4	bidentate
Hg	2.224(1)	2.61(2)	107.9(12)	88.6(12)	0.39	19.3	anisobidentate

[a] The two values are for the two crystallographically independent $\{[\mathrm{Pim}^{\mathrm{Pr^i,Bu^t}}]\mathrm{Cu(NO_3)}\}^+$ ions in $\{[\mathrm{Pim}^{\mathrm{Pr^i,Bu^t}}]\mathrm{Cu(NO_3)}\}_2[\mathrm{Cu(NO_3)_4}]$. [b] Values for $\{[\mathrm{Pim}^{\mathrm{Pr^i,Bu^t}}]\mathrm{Cu(NO_3)}\}(\mathrm{NO_3})$.

Table 9. Classification of Nitrate Coordination Mode for $[\mathrm{M(NO_3)_4}]^{2-}$ Ions

compound	d_1/Å	d_2/Å	Δd/Å	ref
$[\mathrm{AsPh_4}]_2[\mathrm{Zn(NO_3)_4}]$	2.06	2.58	0.52	*c*
$[\{\mathrm{MeNC_3H_6}\}_4]\mathrm{Cd(NO_3)}]_2[\mathrm{Cd(NO_3)_4}]$[a]	2.27	2.57	0.30	*d*
	2.37	2.41	0.04	
$\{[\mathrm{Pim}^{\mathrm{Pr^i,Bu^t}}]\mathrm{Cd(NO_3)}\}_2[\mathrm{Cd(NO_3)_4}]$[b]	2.27(2)	2.31(2)	0.04	this work
	2.38(2)	2.44(2)	0.06	
$\{[\mathrm{Pim}^{\mathrm{Pr^i,Bu^t}}]\mathrm{Hg(NO_3)}\}_2[\mathrm{Hg(NO_3)_4}]$[b]	2.33(2)	2.40(3)	0.07	this work
	2.46(2)	2.57(3)	0.11	

[a] The two values are for two crystallographically independent $[\mathrm{Cd(NO_3)_4}]^{2-}$ ions. [b] The two values are for two crystallographically independent $\mathrm{NO_3}^-$ ligands in each $[\mathrm{M(NO_3)_4}]^{2-}$ ion. [c] Bellitto, C.; Gastaldi, L.; Tomlinson, A. A. G. *J. Chem. Soc., Dalton Trans.* **1976**, 989−992. [d] Alcock, N. W.; Curzon, E. H.; Moore, P.; Pierpoint, C. *J. Chem. Soc., Dalton Trans.* **1984**, 605−610.

Table 10. Activities of $\mathrm{M^{II}}$-Carbonic Anhydrases[a]

M	activity/%	Δd/Å for $\{[\mathrm{Pim}^{\mathrm{Pr^i,Bu^t}}]\mathrm{M(NO_3)}\}^+$
Zn	100	0.53
Co	50	0.27
Cu	0	0.13[b]
Cd	2	0.13
Hg	0	0.39

[a] Data taken from: Bertini, I.; Luchinat, C.; Viezzoli, M. S. In *Zinc Enzymes;* Bertini, I., Luchinat, C., Maret, W., Zeppezauer, M., Eds.; *Progress in Inorganic Biochemistry and Biophysics*, Vol. 1; Birkhäuser: Boston, MA, 1986; Chapter 3. [b] Average values for the three crystallographically independent molecules.

Table 11. Comparison of Nitrate Coordination Modes as a Function of Overall Charge on $\mathrm{LM(NO_3)}^{Q+}$ [a]

	Δd/Å		$\Delta\theta$/deg	
M	$[\mathrm{Pim}^{\mathrm{Pr^i,Bu^t}}]$	$[\mathrm{Tp}^{\mathrm{Bu^t,R}}]$[b]	$[\mathrm{Pim}^{\mathrm{Pr^i,Bu^t}}]$	$[\mathrm{Tp}^{\mathrm{Bu^t,R}}]$[b]
Zn	0.53	0.60	24.4	29.6
Co	0.27	0.34	10.8	15.8
Cd	0.13	0.23	7.4	1.8
Cu[c]	0.13	0	5.9	0

[a] $Q = 1$ for L = $[\mathrm{Pim}^{\mathrm{Pr^i,Bu^t}}]$; $Q = 0$ for L = $[\mathrm{Tp}^{\mathrm{Bu^t,R}}]$. [b] R = H for M = Zn, Co, Cu; R = Me for M = Cd. See: Han, R.; Looney, A.; McNeill, K.; Parkin, G.; Rheingold, A. L.; Haggerty, B. S. *J. Inorg. Biochem.* **1993**, *49*, 105−121. Looney, A.; Saleh, A.; Zhang, Y. H.; Parkin, G. *Inorg. Chem.* **1994**, *33*, 1158−1164. [c] Average values for the three crystallographically independent molecules.

mercury is often anomalous;[35] for example the pK_a of the hydrated $\mathrm{Hg^{2+}}$ ion (3.4) is exceptionally low compared to the values for $\mathrm{Cd^{2+}}$ (10.1) and $\mathrm{Zn^{2+}}$ (9.0).[36,37]

The variation of the nitrate coordination mode within $\{[\mathrm{Pim}^{\mathrm{Pr^i,Bu^t}}]\mathrm{M(NO_3)}\}^+$ correlates with that observed previously for the tris(pyrazolyl)hydroborato complexes $[\mathrm{Tp}^{\mathrm{Bu^t,R}}]\mathrm{M(NO_3)}$ (M = Co, Cu, Zn, Cd).[13,38] Furthermore, direct comparison of the pairs of complexes $\{[\mathrm{Pim}^{\mathrm{Pr^i,Bu^t}}]\mathrm{M(NO_3)}\}^+$ and $[\mathrm{Tp}^{\mathrm{Bu^t,R}}]\mathrm{M(NO_3)}$ demonstrates the effect that the neutral $[\mathrm{Pim}^{\mathrm{Pr^i,Bu^t}}]$ ligand has upon modifying the nitrate coordination mode relative to that of the charged $[\mathrm{Tp}^{\mathrm{Bu^t,R}}]^-$ ligand. Thus, for Zn and Co, the $[\mathrm{Pim}^{\mathrm{Pr^i,Bu^t}}]$ ligand increases the bidenticity of the nitrate ligand in $\{[\mathrm{Pim}^{\mathrm{Pr^i,Bu^t}}]\mathrm{M(NO_3)}\}^+$ compared to that in $[\mathrm{Tp^{Bu^t}}]\mathrm{M(NO_3)}$. In contrast, the bidenticity in the Cu complex $\{[\mathrm{Pim}^{\mathrm{Pr^i,Bu^t}}]\mathrm{Cu(NO_3)}\}^+$ is slightly less than that in $[\mathrm{Tp^{Bu^t}}]\mathrm{Cu(NO_3)}$ (Table 11); however, the departure from symmetric bidentate coordination for $\{[\mathrm{Pim}^{\mathrm{Pr^i,Bu^t}}]\mathrm{Cu(NO_3)}\}^+$ is so small that it is not chemically significant, as indicated by the slight differences in the two crystallographically independent molecules in $\{[\mathrm{Pim}^{\mathrm{Pr^i,Bu^t}}]\mathrm{Cu(NO_3)}\}_2[\mathrm{Cu(NO_3)_4}]$ and that in $\{[\mathrm{Pim}^{\mathrm{Pr^i,Bu^t}}]\mathrm{Cu(NO_3)}\}(\mathrm{NO_3})$ (Table 8).

Finally, it is important to emphasize the obvious importance and challenge of utilizing ligand geometries that create accurate representations of metalloenzyme active sites, since the structural (and hence reactivity) changes observed are very dependent on the nature of the ligand system. For example, of the complexes $\mathrm{M(NC_5H_5)_3(NO_3)_2}$ (M = Co, Cu, Zn), in which the metals are also coordinated to three nitrogen donors, but with a different geometry, it is the copper, rather than zinc, derivative which has the nitrate ligand with the greatest asymmetry, as judged by the difference in M−O bond lengths: Cu (0.578 Å) $\gg$ Zn (0.186 Å) $>$ Co (0.104 Å).[39,40]

---

(34) Rees, D. C.; Howard, J. B.; Chakrabarti, P.; Yeates, T.; Hsu, B. T.; Hardman, K. D.; Lipscomb, W. N. In *Zinc Enzymes*; Bertini, I., Luchinat, C., Maret, W., Zeppezauer, M., Eds.; Progress Inorganic Biochemistry and Biophysics; Vol. 1; Birkhäuser: Boston, MA, 1986; Chapter 10.

(35) The anomalous nature of mercury is often attributed to relativistic effects. See, for example: (a) Pyykkö, P.; Desclaux, J.-P. *Acc. Chem. Res.* **1979**, *12*, 276−281. (b) Pitzer, K. S. *Acc. Chem. Res.* **1979**, *12*, *8*, 271−276. (c) Pyykkö, P. *Chem. Rev.* **1988**, *88*, 563−594.

(36) Smith, R. M.; Martell, A. E. *Critical Stability Constants*; Plenum Press: New York 1976; Vol. 4 (Inorganic Complexes).

(37) A reviewer has suggested that the inactivity of $\mathrm{Hg^{II}}$-carbonic anhydrase may also be due to a low nucleophilicity of the mercury-bound hydroxide inhibiting reaction towards $\mathrm{CO_2}$.

(38) Furthermore, structural comparisons of zinc and cobalt nitrate complexes in other systems indicate that cobalt exhibits the greater preference for bidentate nitrate ligand coordination. See, for example: Dowling, C.; Murphy, V. J.; Parkin, G. *Inorg. Chem.* **1996**, *35*, 2415−2420.

(39) Cameron, A. F.; Taylor, D. W.; Nuttall, R. H. *J. Chem. Soc., Dalton Trans.* **1972**, 1603−1608.

(40) The Cd analogue also possesses bidentate nitrate ligands (asymmetry = 0.047 Å). See: Cameron, A. F.; Taylor, D. W.; Nuttall, R. H. *J. Chem. Soc., Dalton Trans.* **1972,** 1608−1611.

Table 12. NMR Data for {[Pim$^{\mathrm{Pr^i,Bu^t}}$]M(NO$_3$)}$^+$ (in CDCl$_3$)[a]

	Zn	Cd	Hg
^{1}H NMR			
$P[C_3N_2H\{CH(CH_3)_2\}\{C(C\mathit{H}_3)_3\}]_3$	1.35 (s)	1.34 (s)	1.38 (s)
$P[C_3N_2H\{CH(C\mathit{H}_3)_2\}\{C(CH_3)_3\}]_3$	1.52 (d, $^{3}J_{\mathrm{H-H}} = 7$)	1.56 (d, $^{3}J_{\mathrm{H-H}} = 7$)	1.57 (d, $^{3}J_{\mathrm{H-H}} = 6$)
$P[C_3N_2H\{C\mathit{H}(CH_3)_2\}\{C(CH_3)_3\}]_3$	5.59 (d, $^{4}J_{\mathrm{P-H}} = 7$; sept, $^{3}J_{\mathrm{H-H}} = 7$)	5.60 (d, $^{4}J_{\mathrm{P-H}} = 7$; sept, $^{3}J_{\mathrm{H-H}} = 7$)	5.64 (d, $^{4}J_{\mathrm{P-H}} = 7$; sept, $^{3}J_{\mathrm{H-H}} = 6$)
$P[C_3N_2\mathit{H}\{CH(CH_3)_2\}\{C(CH_3)_3\}]_3$	6.98 (d, $^{4}J_{\mathrm{P-H}} = 4$)	7.02 (d, $^{4}J_{\mathrm{P-H}} = 5$; d$_{\mathrm{sat}}$,$^{4}J_{\mathrm{Cd-H}} = 8$)	7.08 (d, $^{4}J_{\mathrm{P-H}} = 5$; d$_{\mathrm{sat}}$,$^{4}J_{\mathrm{Hg-H}} = 26$)
^{13}C NMR			
$P[C_3N_2H\{CH(CH_3)_2\}\{C(\mathit{C}H_3)_3\}]_3$	29.7 (q, $^{1}J_{\mathrm{C-H}} = 127$)	29.6 (q, $^{1}J_{\mathrm{C-H}} = 127$)	29.4 (q, $^{1}J_{\mathrm{C-H}} = 127$)
$P[C_3N_2H\{CH(CH_3)_2\}\{\mathit{C}(CH_3)_3\}]_3$	31.8 (s)	31.5 (s)	31.4 (s)
$P[C_3N_2H\{CH(\mathit{C}H_3)_2\}\{C(CH_3)_3\}]_3$	24.1 (q, $^{1}J_{\mathrm{C-H}} = 128$)	23.9 (q, $^{1}J_{\mathrm{C-H}} = 128$)	24.0 (q, $^{1}J_{\mathrm{C-H}} = 127$)
$P[C_3N_2H\{\mathit{C}H(CH_3)_2\}\{C(CH_3)_3\}]_3$	51.5 (d, $^{1}J_{\mathrm{C-H}} = 145$; d, $^{3}J_{\mathrm{P-C}} = 19$)	51.9 (d, $^{1}J_{\mathrm{C-H}} = 144$; d, $^{3}J_{\mathrm{P-C}} = 20$)	51.9 (d, $^{1}J_{\mathrm{C-H}} = 144$; d, $^{3}J_{\mathrm{P-C}} = 20$)
$P[\mathit{C}_3N_2H\{CH(CH_3)_2\}\{C(CH_3)_3\}]_3$	115.3 (d, $^{1}J_{\mathrm{C-H}} = 194$)	115.3 (d, $^{1}J_{\mathrm{C-H}} = 191$)	115.4 (d, $^{1}J_{\mathrm{C-H}} = 192$)
	139.1 (s)	138.4 (s)	138.3 (s)
	155.8 (s)	155.2 (s)	154.9 (s)
^{31}P{^{1}H} NMR			
	−121.3 (s)	−120 (d$_{\mathrm{sat}}$, $^{3}J_{\mathrm{Cd-P}} = 22$)	−122 (d$_{\mathrm{sat}}$, $^{3}J_{\mathrm{Hg-P}} = 32$)
^{113}Cd NMR			
		169 (d, $^{3}J_{\mathrm{Cd-P}} = 22$)	

[a] Chemical shifts in ppm; *J* values in Hz.

Experimental Section

General Considerations. All manipulations were performed using combinations of glovebox, high-vacuum, and Schlenk techniques.[41] Solvents were purified and degassed by standard procedures. [Pim$^{\mathrm{Pr^i,Bu^t}}$] was prepared by the literature method.[10]

^{1}H NMR spectra were recorded on Varian VXR-400 and Bruker Avance 400 DRX spectrometers. ^{13}C NMR spectra were recorded on Varian VXR-300 (75.43 MHz) and Bruker Avance 300wb DRX (75.47 MHz) spectrometers. ^{31}P NMR spectra were recorded on Varian VXR-300 (121.42 MHz) and Bruker Avance 300wb DRX (121.49 MHz) spectrometers. ^{113}Cd NMR spectra were recorded on a Bruker Avance 300wb DRX (66.57 MHz) spectrometer. ^{1}H and ^{13}C chemical shifts are reported in ppm relative to SiMe$_4$ ($\delta = 0$) and were referenced internally with respect to the protio solvent impurity and the ^{13}C resonances, respectively. ^{113}Cd chemical shifts are referenced relative to 0.1 M aqueous Cd(ClO$_4$)$_2$ ($\delta = 0$), using an external standard of 4.2 M aqueous Cd(ClO$_4$)$_2$ ($\delta = -8.11$ ppm).[42] All coupling constants are reported in Hz. IR spectra were recorded for KBr pellets on Perkin-Elmer 1430 and 1600 spectrophotometers and are reported in cm^{-1}. C, H, and N elemental analyses were determined using a Perkin-Elmer 2400 CHN elemental analyzer.

Synthesis of {[Pim$^{\mathbf{Pr^i,Bu^t}}$]Zn(NO$_3$)}(NO$_3$). A mixture of [Pim$^{\mathrm{Pr^i,Bu^t}}$] (200 mg, 0.38 mmol) and Zn(NO$_3$)$_2$·6H$_2$O (124 mg, 0.42 mmol) was stirred in MeOH (ca. 10 mL). The mixture was filtered after ca. 1 h, and the volatile components were removed from the filtrate in vacuo, giving a white solid, which was extracted into CHCl$_3$ (ca. 10 mL). The solution was concentrated to ca. 5 mL, resulting in the formation of microcrystals. The mixture was cooled to 0 °C and filtered, giving {[Pim$^{\mathrm{Pr^i,Bu^t}}$]Zn(NO$_3$)}(NO$_3$) as a white precipitate (95 mg, 35%), which was dried in vacuo. Anal. Calcd for {[Pim$^{\mathrm{Pr^i,Bu^t}}$]Zn(NO$_3$)}(NO$_3$)·CHCl$_3$: C, 44.6; H, 6.3; N, 13.4. Found: C, 44.3; H, 6.6; N, 13.4. IR data (cm^{-1}, KBr pellet): 3128 (m), 3071 (m), 2971 (vs), 2910 (s), 2873 (s), 1655 (w), 1550 (s), 1523 (s), 1465 (vs), 1430 (vs), 1396 (vs), 1344 (vs), 1291 (vs), 1228 (vs), 1204 (s), 1158 (s), 1135 (m), 1102 (w), 1073 (s), 1015 (s), 936 (vw), 890 (w), 830 (w), 813 (w), 786 (w), 750 (s), 688 (m), 612 (m), 586 (m), 563 (w), 542 (w), 515 (s), 455 (w). NMR spectroscopic data are listed in Table 12.

Synthesis of {[Pim$^{\mathbf{Pr^i,Bu^t}}$]Co(NO$_3$)}(NO$_3$). A mixture of [Pim$^{\mathrm{Pr^i,Bu^t}}$] (200 mg, 0.38 mmol) and Co(NO$_3$)$_2$·6H$_2$O (122 mg, 0.42 mmol) was stirred in MeOH (ca. 5 mL) for ca. 10 min, after which the volatile components were removed in vacuo. The mixture was extracted into CHCl$_3$ (10 mL) and filtered. The filtrate was concentrated to ca. 5 mL and pentane was added to precipitate the product. The mixture was filtered, and the product was washed with pentane to give {[Pim$^{\mathrm{Pr^i,Bu^t}}$]-Co(NO$_3$)}(NO$_3$) as a purple powder (230 mg, 80%). Anal. Calcd for {[Pim$^{\mathrm{Pr^i,Bu^t}}$]Co(NO$_3$)}(NO$_3$)·0.4CHCl$_3$: C, 48.3; H, 6.8; N, 14.8. Found: C, 48.3; H, 6.8; N, 15.2. IR data (cm^{-1}; KBr pellet): 3147 (m), 3069 (w), 2968 (s), 2871 (m), 1560 (m), 1542 (vs), 1522 (s), 1509 (s), 1477 (s), 1460 (s), 1424 (s), 1366 (vs), 1317 (s), 1300 (s), 1280 (s), 1263 (s), 1226 (s), 1198 (s), 1162 (s), 1135 (s), 1074 (vs), 1022 (s), 1008 (s), 933 (w), 890 (w), 802 (m), 785 (m), 755 (w), 732 (w), 690 (m), 662 (vw), 610 (w), 586 (w), 561 (vw), 540 (w), 516 (m), 460 (m). Electronic spectral data in THF [λ/nm (ϵ/M^{-1} cm^{-1})]: 550 (100), 576 (120), 620 (70), 643 (50), 655 (40), 668 (50).

Synthesis of {[Pim$^{\mathbf{Pr^i,Bu^t}}$]Cu(NO$_3$)}$_2$[Cu(NO$_3$)$_4$]. [Pim$^{\mathrm{Pr^i,Bu^t}}$] (100 mg, 0.19 mmol) was added to a solution of Cu(NO$_3$)$_2$·2.5H$_2$O (66 mg, 0.28 mmol) in THF (ca. 5 mL), giving an olive green solution which deposited a gray/green precipitate after ca. 5 min. The mixture was stirred for 75 min at room temperature and filtered. The residue was extracted with additional THF (ca. 15 mL), and the extract was combined with the reaction filtrate. The volatile components were removed in vacuo, and the solid obtained was washed with pentane, giving {[Pim$^{\mathrm{Pr^i,Bu^t}}$]Cu(NO$_3$)}$_2$[Cu(NO$_3$)$_4$] as a pale gray/green powder (42 mg, 25%). Anal. Calcd for {[Pim$^{\mathrm{Pr^i,Bu^t}}$]Cu(NO$_3$)}$_2$[Cu(NO$_3$)$_4$]·2THF: C, 46.4; H, 6.8; N, 14.3. Found: C, 46.6; H, 6.6; N, 14.4. IR data (cm^{-1}; KBr pellet): 3125 (m), 3069 (m), 2969 (vs), 2872 (m), 2715 (vw), 2546 (vw), 2057 (vw), 1746 (vw), 1601 (w), 1534 (vs), 1463 (s), 1434 (s), 1396 (vs), 1348 (vs), 1264 (vs), 1231 (vs), 1201 (m), 1165 (m), 1135 (m), 1106 (vw), 1075 (m), 1018 (s), 933 (vw), 888 (w), 830 (w), 801 (w), 764 (w), 730 (w), 692 (w), 677 (w), 613 (w), 585 (w), 562 (w), 543 (w), 517 (m), 455 (vw), 404 (vw).

Synthesis of {[Pim$^{\mathbf{Pr^i,Bu^t}}$]Cu(NO$_3$)}(NO$_3$). [Pim$^{\mathrm{Pr^i,Bu^t}}$] (500 mg, 0.95 mmol) was added to a solution of Cu(NO$_3$)$_2$·2.5H$_2$O (232 mg, 1.00 mmol) in MeOH (ca. 80 mL), giving a dark green solution. The solution was stirred for ca. 10 min, after which the methanol was removed in vacuo. The residue was extracted into CHCl$_3$ (ca. 30 mL), and the mixture was filtered. The filtrate was concentrated to ca. 5 mL, depositing dark green crystals of {[Pim$^{\mathrm{Pr^i,Bu^t}}$]Cu(NO$_3$)}(NO$_3$)·2CHCl$_3$, which were isolated by filtration and washed with pentane (634 mg, 67%). Anal. Calcd for {[Pim$^{\mathrm{Pr^i,Bu^t}}$]Cu(NO$_3$)}(NO$_3$)·2CHCl$_3$: C, 40.3; H, 5.6; N, 11.8. Found: C, 40.3; H, 5.6; N, 11.7.

Synthesis of {[Pim$^{\mathbf{Pr^i,Bu^t}}$]Cd(NO$_3$)}$_2$[Cd(NO$_3$)$_4$]. A solution of [Pim$^{\mathrm{Pr^i,Bu^t}}$] (300 mg, 0.57 mmol) in CHCl$_3$ (3 mL) was added dropwise to a stirred solution of Cd(NO$_3$)$_2$·4H$_2$O (290 mg, 0.94 mmol) in EtOH (3 mL) at 0 °C. The ice bath was removed and the mixture was stirred for ca. 3 min. The volatile components were removed in vacuo, leaving a white solid that was extracted into CHCl$_3$ (ca. 35 mL). The mixture

---

(41) (a) McNally, J. P.; Leong, V. S.; Cooper, N. J. In *Experimental Organometallic Chemistry*; Wayda, A. L., Darensbourg, M. Y., Eds.; American Chemical Society: Washington, DC, 1987; Chapter 2, pp 6−23. (b) Burger, B. J.; Bercaw, J. E. In *Experimental Organometallic Chemistry*; Wayda, A. L., Darensbourg, M. Y., Eds.; American Chemical Society: Washington, DC, 1987; Chapter 4, pp 79−98. (c) Shriver, D. F.; Drezdzon, M. A. *The Manipulation of Air-Sensitive Compounds*, 2nd ed.; Wiley-Interscience: New York, 1986.

(42) Maciel, G. E.; Borzo, M. *J. Chem. Soc., Chem. Commun.* **1973**, 394.

Table 13. Crystal, Intensity Collection, and Refinement Data for $\{[\mathrm{Pim}^{\mathrm{Pr^i,Bu^t}}]\mathrm{M(NO_3)}\}(\mathrm{NO_3})$ (M = Zn, Co, Cu) and $\{[\mathrm{Pim}^{\mathrm{Pr^i,Bu^t}}]\mathrm{M(NO_3)}\}_2[\mathrm{M(NO_3)_4}]$ (M = Cu, Cd, Hg)

	Co[a]	Zn[a]	Cu[a]	Cu[b]	Cd[b]	Hg[b]
lattice	orthorhombic	triclinic	orthorhombic	triclinic	monoclinic	monoclinic
empirical formula	$C_{32}H_{53}Cl_6N_8O_6PCo$	$C_{22}H_{54}N_9O_6PZn$	$C_{32}H_{53}Cl_6N_8O_6PCu$	$C_{60}H_{102}N_{18}O_{18}P_2Cu_3$	$C_{60}H_{102}N_{18}O_{18}P_2Cd_3$	$C_{60}H_{102}N_{18}O_{18}P_2Hg_3$
fw	948.4	757.2	953.03	1616.2	1762.7	2027.3
space group	*Pnma* (No. 62)	$P\bar{1}$ (No. 2)	*Pnma* (No. 62)	$P\bar{1}$ (No. 2)	*C*2/*c* (No. 15)	*C*2/*c* (No. 15)
a/Å	20.667(7)	10.503(4)	20.427(4)	10.6485(8)	43.191(5)	43.183(5)
b/Å	14.102(2)	13.909(5)	14.050(3)	16.8794(11)	10.361(2)	10.374(2)
c/Å	16.809(4)	14.245(3)	16.569(3)	23.2919(16)	17.614(2)	17.597(3)
α/deg	90	104.19(2)	90	74.158(1)	90	90
β/deg	90	105.39(2)	90	89.587(1)	90.949(7)	91.010(1)
γ/deg	90	91.76(3)	90	75.020(1)	90	90
V/Å^3	4889(2)	1935(1)	4756(2)	3881.6(5)	7881(2)	7881(2)
Z	4	2	4	2	4	4
temp/K	298	298	203	228	298	298
λ, Å	0.710 73	0.710 73	0.710 73	0.710 73	0.710 73	0.710 73
ρ(calcd)/g cm^{-3}	1.286	1.300	1.331	1.383	1.486	1.709
μ(Mo Kα), mm^{-1}	0.76	0.73	0.88	0.93	0.92	5.94
$\theta_{\max}$, deg	22.5	22.5	28.3	28.3	22.5	24.0
no. of data	3459	5021	5724	17128	4804	6120
no. of params	299	431	295	941	457	457
R1	0.0686	0.0481	0.0762	0.0419	0.0730	0.0656
wR2	0.0756	0.0571	0.1939	0.1005	0.1063	0.1378
GOF	1.570	1.350	1.071	1.006	1.030	1.023

[a] $\{[\mathrm{Pim}^{\mathrm{Pr^i,Bu^t}}]\mathrm{M(NO_3)}\}(\mathrm{NO_3})$. [b] $\{[\mathrm{Pim}^{\mathrm{Pr^i,Bu^t}}]\mathrm{M(NO_3)}\}_2[\mathrm{M(NO_3)_4}]$.

was filtered and the solvent was removed in vacuo yielding $\{[\mathrm{Pim}^{\mathrm{Pr^i,Bu^t}}]\mathrm{Cd(NO_3)}\}_2\ [\mathrm{Cd(NO_3)_4}]\cdot 2\mathrm{CHCl_3}$ as a white powder (260 mg, 46%). Anal. Calcd for $\{[\mathrm{Pim}^{\mathrm{Pr^i,Bu^t}}]\mathrm{Cd(NO_3)}\}_2[\mathrm{Cd(NO_3)_4}]\cdot 2\mathrm{CHCl_3}$: C, 37.2; H, 5.2; N, 12.6. Found: C, 37.8; H, 5.6; N, 12.5. IR data (cm^{-1}; KBr pellet): 3426 (w), 3141 (w), 2972 (s), 2936 (m), 2872 (m), 1550 (m), 1519 (vs), 1456 (s), 1366 (s), 1292 (s), 1248 (vs), 1224 (s), 1199 (m), 1176 (m), 1156 (m), 1134 (m), 1101 (m), 1068 (m), 1028 (m), 1012 (s), 932 (vw), 889 (w), 818 (m), 807 (m), 788 (m), 742 (vw), 729 (w), 685 (w), 606 (m), 584 (m), 560 (w), 539 (w), 512 (m), 454 (vw), 411 (vw). NMR spectroscopic data are listed in Table 12.

Synthesis of $\{[\mathrm{Pim}^{\mathrm{Pr^i,Bu^t}}]\mathrm{Hg(NO_3)}\}_2[\mathrm{Hg(NO_3)_4}]$. $\mathrm{Hg(NO_3)_2\cdot H_2O}$ (128 mg, 0.37 mmol) was added to a solution of $[\mathrm{Pim}^{\mathrm{Pr^i,Bu^t}}]$ (125 mg, 0.24 mmol) in MeOH (ca. 8 mL). The mixture was stirred overnight and filtered. The solvent was removed from the filtrate in vacuo, giving a white powder, which was washed with pentane (ca. 10 mL), yielding $\{[\mathrm{Pim}^{\mathrm{Pr^i,Bu^t}}]\mathrm{Hg(NO_3)}\}_2[\mathrm{Hg(NO_3)_4}]$ (194 mg, 80%). Anal. Calcd for $\{[\mathrm{Pim}^{\mathrm{Pr^i,Bu^t}}]\mathrm{Hg(NO_3)}\}_2[\mathrm{Hg(NO_3)_4}]$: C, 35.6; H, 5.1; N, 12.4. Found: C, 35.4; H, 5.2; N, 12.0. IR data (cm^{-1}; KBr pellet): 3139 (m), 2972 (vs), 2936 (s), 2871(m), 1548 (s), 1520 (vs), 1459 (vs), 1366 (vs), 1272 (vs), 1224 (vs), 1199 (s), 1176 (s), 1156 (s), 1134 (s), 1101 (w), 1068 (s), 1013 (s), 982 (s), 933 (w), 889 (w), 813 (m), 797 (w), 787 (w), 726 (w), 686 (m), 606 (m), 584 (m), 560 (w), 540 (w), 511 (m), 458 (vw), 414 (vw). NMR spectroscopic data are listed in Table 12.

X-ray Structure Determinations. Crystal data, data collection and refinement parameters for $\{[\mathrm{Pim}^{\mathrm{Pr^i,Bu^t}}]\mathrm{Zn(NO_3)}\}(\mathrm{NO_3})$, $\{[\mathrm{Pim}^{\mathrm{Pr^i,Bu^t}}]\mathrm{Co(NO_3)}\}(\mathrm{NO_3})$, $\{[\mathrm{Pim}^{\mathrm{Pr^i,Bu^t}}]\mathrm{Cu(NO_3)}\}(\mathrm{NO_3})$, $\{[\mathrm{Pim}^{\mathrm{Pr^i,Bu^t}}]\mathrm{Cu(NO_3)}\}_2[\mathrm{Cu(NO_3)_4}]$, $\{[\mathrm{Pim}^{\mathrm{Pr^i,Bu^t}}]\mathrm{Cd(NO_3)}\}_2[\mathrm{Cd(NO_3)_4}]$, and $\{[\mathrm{Pim}^{\mathrm{Pr^i,Bu^t}}]\mathrm{Hg(NO_3)}\}_2[\mathrm{Hg(NO_3)_4}]$ are summarized in Table 13. X-ray diffraction data for $\{[\mathrm{Pim}^{\mathrm{Pr^i,Bu^t}}]\mathrm{Zn(NO_3)}\}(\mathrm{NO_3})$, $\{[\mathrm{Pim}^{\mathrm{Pr^i,Bu^t}}]\mathrm{Co(NO_3)}\}(\mathrm{NO_3})$, $\{[\mathrm{Pim}^{\mathrm{Pr^i,Bu^t}}]\mathrm{Cd(NO_3)}\}_2[\mathrm{Cd(NO_3)_4}]$, and $\{[\mathrm{Pim}^{\mathrm{Pr^i,Bu^t}}]\mathrm{Hg(NO_3)}\}_2[\mathrm{Hg(NO_3)_4}]$ were collected on a Siemens P4 diffractometer. The unit cells were determined by the automatic indexing of 25 centered reflections and confirmed by examination of the axial photographs. Intensity data were collected using graphite-monochromated Mo Kα X-radiation ($\lambda = 0.710\ 73$ Å). Check reflections were measured every 100 reflections, and the data were scaled accordingly and corrected for Lorentz, polarization, and absorption effects. X-ray diffraction data for $\{[\mathrm{Pim}^{\mathrm{Pr^i,Bu^t}}]\mathrm{Cu(NO_3)}\}(\mathrm{NO_3})$ and $\{[\mathrm{Pim}^{\mathrm{Pr^i,Bu^t}}]\mathrm{Cu(NO_3)}\}_2[\mathrm{Cu(NO_3)_4}]$ were collected on a Bruker P4 diffractometer equipped with a SMART CCD detector. The structures were solved using direct methods and standard difference map techniques and were refined by full-matrix least-squares procedures using SHELXTL.[43] Hydrogen atoms on carbon were included in calculated positions. Atomic coordinates for $\{[\mathrm{Pim}^{\mathrm{Pr^i,Bu^t}}]\mathrm{Zn(NO_3)}\}(\mathrm{NO_3})$ and $\{[\mathrm{Pim}^{\mathrm{Pr^i,Bu^t}}]\mathrm{Co(NO_3)}\}(\mathrm{NO_3})$ have been deposited with the Cambridge Crystallographic Data Center.[8,9]

Summary

With the exception of that in the $\mathrm{Hg^{II}}$ derivative, the nitrate ligand coordination modes in $\{[\mathrm{Pim}^{\mathrm{Pr^i,Bu^t}}]\mathrm{M(NO_3)}\}^+$ correlate with the activity of metal-substituted carbonic anhydrases. Thus, the only $\mathrm{M^{II}}$-carbonic anhydrases which exhibit significant activity, i.e., the Zn and Co species, are those for which $\{[\mathrm{Pim}^{\mathrm{Pr^i,Bu^t}}]\mathrm{M(NO_3)}\}^+$ possesses a markedly asymmetric nitrate ligand. This trend supports the notion that access to a unidentate, rather than a bidentate, bicarbonate intermediate may be a critical requirement for carbonic anhydrase activity. The correlation between nitrate coordination mode and enzyme activity is anomalous for mercury, since $\mathrm{Hg^{II}}$-carbonic anhydrase is inactive but yet $\{[\mathrm{Pim}^{\mathrm{Pr^i,Bu^t}}]\mathrm{Hg(NO_3)}\}^+$ possesses a unidentate nitrate ligand. Therefore, it is suggested that the inactivity of $\mathrm{Hg^{II}}$-carbonic anhydrase may be a consequence of the reduced tendency of the mercury center in $\mathrm{Hg^{II}}$-carbonic anhydrase to bind water in preference to other ligands. Finally, comparison of the structure of $\{[\mathrm{Pim}^{\mathrm{Pr^i,Bu^t}}]\mathrm{Zn(NO_3)}\}^+$ with that of its neutral counterpart $[\mathrm{Tp^{Bu^t}}]\mathrm{ZnNO_3}$ demonstrates that the charged complex exhibits a more pronounced tendency to adopt bidentate coordination of the nitrate ligand. In view of the similar steric demands of the two ligand systems, the fine-tuning that is necessary to create synthetic analogues which accurately mimic the chemistry of metalloenzymes is emphasized.

Acknowledgment. We thank the National Institutes of Health (Grant GM46502) for support of this research and the reviewers for valuable comments.

Supporting Information Available: Listings of X-ray experimental details, atomic coordinates, thermal parameters, bond distances, and bond angles and additional ORTEP diagrams. This material is available free of charge via the Internet at http://pubs.acs.org.

IC990682V

---

(43) Sheldrick, G. M. *SHELXTL: An Integrated System for Solving, Refining and Displaying Crystal Structures from Diffraction Data*; University of Göttingen: Göttingen, Germany, 1981.